Capillary zone electrophoresis determination of aniline and pyridine in sewage samples using transient isotachophoresis with a system-induced terminator

Hattori, Takanari
Okamura, Hideo
Asaoka, Satoshi
Fukushi, Keiichi

(Citation)
Journal of Chromatography A,1511:132-137

(Issue Date)
2017-08-18

(Resource Type)
journal article

(Version)
Accepted Manuscript

(URL)
https://hdl.handle.net/20.500.14094/90004294

Capillary zone electrophoresis determination of aniline and pyridine in sewage samples using transient isotachophoresis with a system-induced terminator

Takanari Hattori, H. Okamura, S. Asaoka, Keiichi Fukushi*

Kobe University Graduate School of Maritime Sciences, 5-1-1 Fukaeminami-machi, Higashinada-ku, Kobe 658-0022, Japan

Correspondence: Dr. Keiichi Fukushi, Kobe University Graduate School of Maritime Sciences, 5-1-1 Fukaeminami-machi, Higashinada-ku, Kobe 658-0022, Japan (Tel. & Fax: +81-78-411-3043; E-mail: fukushi@maritime.kobe-u.ac.jp)

Abstract

Transient isotachophoresis (tITP) with a system-induced terminator (SIT) was developed for capillary zone electrophoresis (CZE) determination of aniline (An^+) and pyridine (Py^+) in sewage samples. After sample injection, a water vial anode was set at the sample-inlet side. Then voltage was applied to generate a system-induced terminator (H^+). Experiments and simulations revealed a concentration effect by tITP with an SIT: background electrolyte (BGE) – 100 mM acetic acid (AcOH) and 50 mM NaOH (pH 4.6); detection wavelength – 200 nm for An^+ and 254 nm for Py^+; vacuum injection period – 15 s (190 nL); SIT generation – 10 kV applied for 80 s with the sample inlet side anode; separation voltage – 20 kV with the sample inlet side anode. The limits of detection (LODs, S/N = 3) of An^+ and Py^+ respectively reached 10 and 42 μg/L, with good repeatability (peak area RSDs ≤ 6.9%) and calibration graph linearity (R^2 = 0.9997). The proposed method was applied for determination of An^+ and Py^+ in sewage samples. Recoveries of An^+ (0.50 mg/L) and Py^+ (2.0 mg/L) in spiked sewage samples were 94–104%.

Keywords: CE; Catiogenic weak electrolyte; Environmental water; On-line concentration; System-induced terminator; Transient isotachophoresis

1. Introduction

Aniline (An^+) is an important raw material used in diverse areas of manufacturing to produce dyes, pigments, paint, pesticides, drugs, plastics, and rubber. Its toxicity and carcinogenicity present risks of various health issues and environmental problems. For that reason, some methods have been developed to treat wastewater containing An^+ [1,2]. Industrial wastewater, agricultural runoff, and urban sewage often contain An^+. For example, concentrations of An^+ in wastewater at shale oil manufacturing sites are reportedly 0.57–14 mg/L [3]. Therefore, increasing attention has been devoted to the monitoring of An^+ concentrations in environmental waters, including wastewater. The most common techniques for the determination of An^+ in environmental waters and wastewater are gas chromatography (GC) [4] and high-performance liquid chromatography (HPLC) [5]. Gas chromatography – mass spectrometry (GC-MS) [6] and CE [7] have also been used. Most methods require sample pretreatment of some type because of the low concentrations of An^+ in samples. Similarly, pyridine (Py^+) is used widely as an important industrial starting material in various industries. It is also used as a solvent and an intermediate in drug and paint industries and as a catalyst in pharmaceutical production. Actually, Py^+ is a highly toxic compound with an unpleasant smell. It is difficult for it to be decomposed by microorganisms in the environment. Concentrations of Py^+ in wastewater from a pharmaceutical plant have been reported as 20–300 mg/L [8]. The regulatory level of Py^+ in wastewater was restricted to 5 mg/L by the United States Environmental Protection Agency (EPA). Quantifying Py^+ in environmental waters, including

wastewaters, is important. Analytical methods such as GC [9], GC-MS [10], HPLC [11], and LC-MS [12] have been used conventionally to quantify concentrations of Py^+.

Compared to other separation methods described above, CE presents several benefits that include high-resolution and environmental compatibility with minimum reagent and sample consumption. However, the concentration sensitivity of CE with conventional UV detection is not sufficiently high because of the-small sample-injection volume and the short light pathway. Therefore, various on-line concentration procedures have been developed to improve the sensitivity: field-amplified sample injection (FASI) [13–17], large volume sample stacking [18,19], dynamic pH junction [20–22], sweeping [23,24], electrokinetic supercharging (EKS) [25–27], and transient isotachophoresis (tITP) [17,28]. Although FASI and EKS are effective for low conductivity samples, they are inapplicable to high-conductivity samples because the analyte transference number decreases concomitantly with increasing matrix concentrations when the sample is injected electrokinetically. Larger volumes of high conductivity samples, however, can be injected in tITP [29]. In such cases, some matrix ions act as the leading or terminating ion [30]. We reported earlier that tITP is useful to concentrate minor components (e.g., nitrite, nitrate, phosphate, and bromate) in seawater [29,31,32].

In this study, tITP using water instead of an external terminating electrolyte was developed as an on-line concentration procedure for capillary zone electrophoresis (CZE) determination of An^+ and Py^+ in sewage samples. We designate this method as tITP with a system-induced terminator (SIT) [33].

Experiments and computer simulations were conducted to ascertain the concentration effects by tITP with an SIT. The sample-injection time, the co-ion and counter-ion concentrations in the background electrolyte (BGE) and the SIT-generation time were optimized. After optimization, the proposed method was applied to quantify concentrations of An^+ and Py^+ in sewage samples.

2. Materials and methods

2.1. tITP with an SIT

A schematic diagram for tITP with an SIT is presnted in Fig. 1. It shows the process: Fill the capillary with a BGE consisting of Na^+ as co-ion and acetic acid (AcO^-) as counter-ion. Vacuum-inject a sample containing An^+ and Py^+ with the sample matrix (Na^+ and Cl^-) (Fig. 1(A)). After replacing the sample vial with a water vial, apply voltage with the sample inlet side as the anode for the specified time (Fig. 1(B)). Migration of Na^+, An^+, and Py^+ to the cathode and that of AcO^- and Cl^- to the anode result in a sample-vacancy zone (SVZ) (Figs. 1(B), 1(C)). In the SVZ, the AcO^- concentration increases because AcO^- migrates continuously from the BGE through the front end of the sample zone. To fulfill the electroneutrality requirement, H^+ is generated from water in the SVZ. It reacts with AcO^-. Deviation of the acid–base balance reduces H^+ effective mobility. The order of effective mobility becomes $Na^+ > Py^+ > An^+ > H^+$. Analytes sandwiched between Na^+ (leading ion) and H^+ (terminating ion) were concentrated by tITP.

After replacing the water vial with the BGE vial, the applied voltage allows to achieve separation and detection of the analytes (Fig. 1(D)).

The difference between EKS with an SIT and the proposed tITP is the following. The former is an electrokinetic sample injection procedure followed by ITP stacking, whereas the latter is a kind of on-line concentration procedure. In addition, a sample is expected to have few coexisting components in EKS: otherwise an SIT cannot be generated. The proposed tITP, in contrast, is applicable to samples for which EKS cannot be used. However, the generation mechanism of an SIT in the proposed tITP is the same as that in EKS [24]. The following benefits of the proposed tITP compared to a conventional tITP can be expected. In the former, water is used as if it is a terminating electrolyte, whereas a terminating electrolyte that contains impurities should be prepared in advance for the latter. Therefore, interference from the impurities can be avoided in the proposed tITP. Labor and time for the preparation of the terminating electrolyte can also be-saved.

2.2. Apparatus

All experiments were conducted using a CE instrument equipped with a photodiode array detector (CAPI-3200; Otsuka Electronics, Osaka, Japan). A polyimide-coated fused-silica capillary (GL Sciences, Tokyo, Japan) with 62.4 cm total length (50 cm effective length) and 50 μm I.D. (375 μm O.D.) was used. The capillary was thermostated at 25°C. The detection wavelength was set at 200 nm

for An+ and 254 nm for Py^+. This experiment used a pH meter (F-22; Horiba, Kyoto, Japan) and a conductivity meter (DS-71; Horiba).

2.3. Chemicals and reagents

All reagents used were of analytical-reagent grade. 6-Aminohexanoic acid, acetic acid (AcOH), An^+, NaCl, NaOH, and Py^+ were obtained from Nacalai Tesque (Kyoto, Japan). BGEs were a mixture of AcOH and NaOH. A stock solution of An^+ and Py^+ was prepared in water at a concentration of 1000 mg/L. It was serially diluted to prepare standard solutions. Sewage samples, before (S1) and after treatment (S2), were taken from a sewage treatment plant near our university. All solutions, including the sewage samples, were filtered through a 0.45 μm membrane filter (Advantec Toyo Kaisha, Tokyo, Japan) before use. Distilled, demineralized water, obtained from an automatic still (WG220; Yamato Kagaku, Tokyo, Japan) and a Simpli Lab-UV high purity water apparatus (Merck Millipore, Tokyo, Japan) was used throughout.

2.4. Experimental procedure

The An^+ and Py^+ spiked to sewage samples were evaluated using the following procedure. No pretreatment procedure was necessary except for adjustment of the sample conductivity to 100 mS/m (by dilution with water or by adding 10,000 mg/L NaCl, if necessary). A new capillary was flushed with water for 5 min, then with 1 M NaOH for 20 min, water for 10 min, and BGE (a mixture

of 100 mM AcOH and 50 mM NaOH, pH 4.6) for 10 min (vacuum pressure, 50 kPa). Before the first analysis conducted each day, the capillary was flushed with water for 5 min and the BGE for 10 min. After the capillary was filled with the BGE, the sample solution was vacuum-injected (50 kPa) for 15 s (190 nL) into the CE apparatus. A water vial was set at the sample-inlet side. Then voltage (10 kV) was applied for 80 s with the sample-inlet side as the anode for SIT generation. Then, the water vial was replaced with the BGE vial. Voltage (25 kV) was applied for separation with the sample-inlet side as the anode. Between runs, the capillary was flushed with the BGE for 3 min. At the end of the day, the capillary was flushed with water for 5 min to fill the capillary with water.

2.5. Computer simulation

To investigate the concentration effect by tITP with an SIT, a computer simulation was performed using Simul 5 Complex software, originally developed by the Gaš group [34,35]. The simulation was conducted on a personal computer (Core i7 2.4 GHz processor; Intel, CA, USA). For the simulation, the total capillary length, I.D. of the capillary, the sample-plug length, the water-plug length, and the space step were set, respectively, as 50 mm, 50 µm, 1 mm, 1 mm, and 5 µm. The BGE was a mixture (pH = 4.8) of 40 mM AcOH (pK_a = 4.756, μ_{lim} = -42.4 × 10^{-9} $m^2V^{-1}s^{-1}$) and 20 mM NaOH (pK_a = 13.7, μ_{lim} = 51.9 × 10^{-9} $m^2V^{-1}s^{-1}$). A sample was a mixture of 0.0537 mM (5 mg/L) An^+ (pK_a = 4.596, μ_{lim} = 30.0 × 10^{-9} $m^2V^{-1}s^{-1}$), 0.0632 mM (5 mg/L) Py^+ (pK_a = 5.18, μ_{lim} = 30.0 × 10^{-9} $m^2V^{-1}s^{-1}$), 7.91 mM NaOH, and 7.91 mM HCl (μ_{lim} (Cl^-) = -79.1 × 10^{-9} $m^2V^{-1}s^{-1}$). NaOH

and HCl were added to adjust the sample conductivity to 100 mS/m. Voltage (100 V) was applied for 50 s with the sample-inlet side as the anode. No electroosmotic flow (EOF) was assumed.

3. Results and discussion

3.1. On-line concentration by tITP with an SIT

A standard solution containing 5 mg/L An^+ and Py^+, adjusted to conductivity 100 mS/m with 10,000 mg/L NaCl, was analyzed to investigate the concentration effect by tITP with an SIT. The BGE was a mixture of 40 mM AcOH and 20 mM NaOH (pH 4.6). After sample injection (50 kPa for 1 s, 13 nL), water vial was set at the sample-inlet side. Voltage was applied for 50 s. Then, the water vial was replaced with the BGE vial. The separation was started according to the procedure described in Section 2.4. The same samples were also analyzed without tITP. Figure 2 portrays the effects of tITP with an SIT. When tITP was not used, the An^+ peak at 200 nm was divided into two peaks -because of insufficient stacking effect- (Fig. 2(A)). When tITP with an SIT was used, the sharper An^+ and Py^+ peaks were obtained respectively at 200 and 254 nm (Fig. 2(B)). The An^+ peak height at 200 nm was ca. 29 fold higher than that at 254 nm. The Py^+ peak height at 254 nm was ca. 1.3-fold higher than that at 200 nm. Therefore, 200 and 254 nm were adopted respectively as the detection wave-lengths for An^+ and Py^+. Both peak heights obtained with the concentration effect were ca. 2.1-fold higher than those without tITP.

Experimentally obtained results were confirmed using computer simulations. Figure 3 presents simulation results of concentration profiles for AcO^-, Na^+, Cl^-, An^+, and Py^+, potential gradient profile, and pH profile in the water, the sample, the BGE zones, and the SVZ. In that figure, panels (A) and (C) depict the distributions at 0 s; panels (B) and (D) portray the distributions at 50 s after voltage was applied. As depicted in Fig. 3(B), AcO^- concentration in the SVZ increased because AcO^- migrated continuously from the BGE zone. No Na^+ or Cl^- was left in the SVZ because they had migrated respectively to the cathode and the anode. Results show that H^+ was generated in the SVZ to fulfill the electroneutrality requirement. This phenomenon appeared as the low pH and high potential gradient in the SVZ (Fig. 3(D)). At the same time, effective mobility of H^+ decreased because of deviation of the acid–base balance with AcO^-. Consequently, H^+ and Na^+ acted respectively as the terminating ion and leading ion to concentrate An^+ and Py^+ between the BGE zone and the SVZ by tITP (Fig. 3(B)).

3.2. Concentrations of co-ions and counter-ions in BGE

The concentrations of co- (Na^+) and counter-ions (AcO^-) in the BGE were varied to assess the effects on enrichment by tITP with an SIT: mixtures of 5–100 mM NaOH and 10–200 mM AcOH, e.g. 5 mM NaOH+10 mM AcOH as BGE. When the concentrations were changed, the capillary was flushed with the same BGE for 10 min. A mixture of 0.50 mg/L An^+ and 2.0 mg/L Py^+, adjusted to conductivity 100 mS/m with 10,000 mg/L NaCl, was analyzed similarly as

described in Section 3.1. In spite of the different concentrations, no significant difference was found in the peak areas and peak heights of An^+ and Py^+ in any BGEs (five combinations of NaOH and AcOH; data not shown). Although the migration-time repeatability improved with increasing BGE concentration, the baseline fluctuation increased when a mixture of 100 mM NaOH and 200 mM AcOH was used. It can therefore be presumed that a mixture of 50 mM NaOH and 100 mM AcOH is a suitable combination for use as BGE.

Considered from Fig. 1, different enrichment behavior can be expected depending on the counter-ion (AcO^-) concentrations. The concentrations of AcO^- was varied (100–500 mM) with fixed concentration of co-ion (Na^+, 50 mM). The mixture of An^+ and Py^+ was analyzed using the procedure described above. The peak area and peak height of An^+ decreased with increased concentration of AcO^- (Fig. S1). The decreasing tendency was the result of the baseline rise because of the UV absorption of AcO^- at 200 nm. The peak area and peak height of Py^+ tended to increase slightly with increasing concentration of AcO^- (Fig. S1). It can be presumed that the increasing tendency is the effect of stronger tITP with higher AcO^- concentration. Additionally, pyridine was detected at 254 nm where little UV absorption by AcO^-. When the AcO^- concentrations were 100, 200, 300, and 500 mM, the respective RSDs (n = 4) of migration time for An^+ and Py^+ were 0.26, 1.2, 0.68, and 1.3% and 0.22, 1.1, 0.60, and 0.84%. Therefore, the optimum BGE adopted in the subsequent experiments was a mixture of 50 mM NaOH and 100 mM AcOH.

260 *3.3. Sample-injection time and SIT-generation time*

261

262 The sample-injection time was varied between 1 and 20 s with the SIT-
263 generation time fixed to 50 s (10 kV). When the standard solution was analyzed,
264 both peak heights of An^+ and Py^+ increased with the sample-injection time up to
265 15 s (data not shown). When the injection time was 20 s, the An^+ peak could not
266 be separated from the SIT peak observed behind the An^+ peak. Therefore, the
267 optimum sample-injection time adopted in the subsequent experiments was 15 s
268 (190 nL). The SIT-generation time was also varied (10–100 s) with the voltage
269 fixed to 10 kV. Both An^+ and Py^+ peak heights increased with the SIT-generation
270 time up to 80 s (data not shown). When the generation time was 100 s, the An^+
271 peak could not be separated from the SIT peak. Therefore, the SIT-generation
272 time adopted in the subsequent experiments was 80 s.

273 Under optimal conditions, the limits of detection (LODs, S/N = 3) for An^+
274 and Py^+ were, respectively, 10 and 42 μg/L. The LODs were improved,
275 respectively, to 17 and 14 times compared to those (170 μg/L for An^+ and 600
276 μg/L for Py^+) obtained using the conventional CZE. Kim et al. [33] reported 3.2
277 times lower LOD (3.1 μg/L) for An^+ than that for our method although the method
278 was not applied to real samples. The limits of quantification (LOQs, S/N = 10) for
279 An^+ and Py^+ were, respectively, 34 and 140 μg/L. The RSDs (n = 4) of migration
280 times for An^+ (0.50 mg/L) and Py^+ (2.0 mg/L) were obtained respectively as 0.46
281 and 0.40%, for peak areas of 4.3 and 3.4%, and for peak heights of 3.4 and 4.4%.

282 To compare the concentration effect by the proposed tITP with that for a
283 conventional tITP, the following experiment was conducted. After the sample was

vacuum-injected for 15 s (190 nL), a terminating electrolyte (100 mM 6-aminohexanoic acid adjusted to pH 4.6 with AcOH) was vacuum-injected for 0.2 s (2.6 nL). The LOD for Py^+ using the proposed tITP was 2.6 times lower than that (110 μg/L) for the conventional tITP, although no significant improvement was found in the LOD for An^+ (12 μg/L for the conventional tITP). According to the simulation results, when AcOH was used as the terminating electrolyte, the maximum concentrations for An^+ and Py^+ were higher and the time required to reach the maximum concentrations were shorter than those for the proposed tITP (data not shown). To compare the concentration effect by the proposed tITP with that for a tITP using AcOH as the terminating electrolyte, the following experiment was conducted. After the sample was vacuum-injected for 15 s, a terminating electrolyte (100 mM AcOH) was vacuum-injected for 3 s or electrokinetically injected for 80 s at 10 kV. The LODs for An^+ and Py^+ for the former were 14 and 50 μg/L and for the latter were 9.7 and 38 μg/L, respectively. The LODs for the proposed tITP were slightly better than those for vacuum injection of AcOH; almost same for those obtained using electrokinetic injection of AcOH.

In the proposed tITP, water introduced into the capillary by EOF during SIT generation might cause some interference with analyte enrichment. Therefore, the water amount was obtained multiplying by the magnitude of EOF (μ_{EOF}, 29.7×10^{-9} $m^2V^{-1}s^{-1}$), SIT-generation time (80 s), the electric field strength in the sample zone (616 V/m), and the cross-sectional area of the capillary (1.96×10^{-15} m^2). The μ_{EOF} was calculated using the water dip observed in an electropherogram as the neutral marker. The electric field strength in the sample zone was obtained

using Simul 5 Complex software. As a result, the water amount was 2.9 nL (1/66 of the sample volume). As described above, the LODs for the proposed tITP were slightly better or same compared to those for the conventional tITP. It was revealed that the negligible quantity did not interfere with the concentration process in the proposed tITP.

In addition to the slightly better LODs, the proposed tITP has the following advantages compared to the conventional tITP as mentioned in Section 2.1. The proposed tITP does not require preparing a terminating electrolyte because a terminator is generated inside the capillary spontaneously. That is to say, the proposed tITP saves costs, time, and labor. On the other hand, when low concentration of analyte is determined using the conventional tITP, some impurities derived from a terminating electrolyte can cause significant blank values. For example, we developed tITP procedure for the determination of nitrite and nitrate in seawater using sodium acetate as the terminating electrolyte [31]. It was necessary to find out sodium acetate with less impurity (nitrite and nitrate) to suppress the blank values. There is no need to worry about the contamination by impurities from a terminating electrolyte for the proposed tITP.

3.4. Sample conductivity

In general, sample conductivity affects the separation and concentration of analytes. The conductivity of sewage samples probably vary according to the sample characteristics. The sample conductivity can affect the separation behavior and concentration degree of An^+ and Py^+. To investigate the effect of sample

conductivity, the conductivity of sample solutions containing 0.50 mg/L An^+ and 2.0 mg/L Py^+ was varied between 50 mS/m and 1,000 mS/m with 10,000 mg/L NaCl. When the sample conductivity was 50 mS/m, An^+ and Py^+ were not separated. The analytes reached the detector before separation was achieved because of the large EOF in the sample zone. The peak area and peak height of An^+ and Py^+ decreased concomitantly with increasing sample conductivity (Fig. S2) because the stacking effect decreased concomitantly with increasing sample conductivity. Therefore, the conductivity of both standard solutions and sewage samples (if necessary) should be adjusted to 100 mS/m in the proposed method.

3.5. Application to sewage samples

Calibration graphs were prepared by analyzing the standard solutions of 0.050–2.5 mg/L An^+ and 0.20–10 mg/L Py^+ (conductivity was adjusted to 100 mS/m with 10,000 mg/L NaCl). Regression equations relating the area response to concentration for An^+ and Py^+ were, respectively, $y = 40.0x + 0.340$ ($R^2 = 0.9997$) and $y = 9.79x + 0.421$ ($R^2 = 0.9997$). Sewage samples spiked with An^+ (0.050 mg/L) and Py^+ (0.20 mg/L) were analyzed using the proposed procedure. It should be noted that An^+ and Py^+ were not detected in the raw sewage samples. The original conductivities of the sewage samples S1 (before treatment) and S2 (after treatment) were, respectively, 106 and 130 mS/m. Therefore, the conductivity of the samples was adjusted to 100 mS/m by diluting with water before analysis. Figure 4 depicts electropherograms of the sewage samples. The RSDs ($n = 4$) of the migration times for An^+ and Py^+ in the sample S1 were obtained respectively

as 0.55 and 0.44%, for peak areas of 3.8 and 3.9%, and for peak heights of 3.0 and 1.9%. The RSDs (n = 4) of the migration times for An^+ and Py^+ in the sample S2 were obtained respectively as 0.50 and 0.29%, for peak areas of 6.9 and 3.2%, and for peak heights of 6.5 and 3.9%. The recoveries of An^+ and Py^+ spiked into the sewage samples S1 and S2 were, respectively, 98 and 88%, and 88 and 111%. Recovery interval of Py^+ (88–111%) was broader compared to that of An^+ (88–98%). It was thought that this interval resulted from the higher LOQ for Py^+ (140 μg/L) than that for An^+ (34 μg/L). Therefore, standard addition experiments were conducted similarly using the same samples containing 10 times more amounts of An^+ (0.50 mg/L) and Py^+ (2.0 mg/L). The recoveries of An^+ and Py^+ were 99–104% and 94–96%, respectively. These results imply that there is no interference with coexisting substances in the sewage samples for the proposed procedure.

The proposed method has sufficient sensitivity for An^+ and Py^+ in the wastewaters and the regulatory level of Py^+ described in Introduction. However, even this sensitive method could not detect An^+ and Py^+ in the raw sewage samples, as mentioned above. In addition, it has been reported that acute toxicity of An^+ to a crustacean (*Daphnia magna*) is 0.040–0.119 mg/L as the median lethal concentration (LC_{50}) [36]; acute toxicity of Py^+ to an alga (*Pseudokirchneriella subcapitata*) is 0.041–0.120 mg/L as the LC_{50} [37]. Therefore, sensitive or more sensitive methods are desired to deal with above matters.

4. Conclusions

We developed a new tITP with an SIT as an online concentration procedure for CZE determination of An^+ and Py^+ in sewage samples. The proposed procedure requires no external terminating electrolyte used for conventional tITP. Therefore, no risk of contamination exists from a terminating electrolyte. Moreover, the procedure saves time and trouble related to preparation of the terminating electrolyte. The LODs of An^+ and Py^+ were improved respectively 17 and 14 times compared to those obtained using the conventional CZE method. The proposed method has sufficient detection power and precision for the determination of sub milligram per liter concentrations of An^+. This report is the first of the relevant literature describing a study of SIT used as the terminating ion in tITP as a CZE concentration procedure.

References

[1] Z. Gu, M. Gao, Z. Luo, L. Lu, Y. Ye, Y. Liu, Bis-pyridinium dibromides modified organo-bentonite for the removal of aniline from wastewater: A positive role of π - π polar interaction, Appl. Surf. Sci. 290 (2014) 107–115.

[2] Y. Gu, H. Qianb, J. Guo, S. Yang, X. Wang, S. Wang, Y. Fu, Synthesis of acidified palygorskite/BiOI with exceptional performances of adsorption and visible-light photoactivity for efficient treatment of aniline wastewater, Appl. Clay Sci. 114 (2015) 124–132.

[3] S. B. Hawthorne, R. E. Sievers, Emission of organic air pollutants from shale oil wastewaters, Appl. Clay Sci. 18 (1984) 483–490.

[4] Y. Y. Han, L. Y. Wang, Y. Y. Zhao, Y. Q. Li, L. Y. Liu, Determination of anilines and toluidines in water by salt-assisted dispersive liquid–liquid microextraction combined with GC-FID, Chromatographia 76 (2013) 1747–1753.

[5] J. F. Jen, C. T. Chang, T. C. Yang, On-line microdialysis–high-performance liquid chromatographic determination of aniline and 2-chloroaniline in polymer industrial wastewater, J. Chromatogr. A 930 (2001) 119–125.

[6] C. P. Diao, C. H. Wei, Rapid determination of anilines in water samples by dispersive liquid–liquid microextraction based on solidification of floating organic drop prior to gas chromatography–mass spectrometry, Anal. Bioanal. Chem. 403 (2012) 877–-884.

[7] S. Liu, W. Wang, J. Chen, J. Sun, Determination of aniline and its derivatives in environmental water by capillary electrophoresis with on-line concentration, Int. J. Mol. Sci. 13 (2012) 6863–6872.

[8] D. H. Lataye, I. M. Mishra, I. D. Mall, Removal of pyridine from aqueous solution by adsorption on bagasse fly ash, Ind. Eng. Chem. Res. 45 (2006) 3934–3943.

[9] J. Macák, V. M. Nabivach, P. Buryan, J. S. Berlizov, Analysis of pyridine bases isolated from a high-temperature coal tar by capillary gas chromatography, J. Chromatogr. A 209 (1981) 472–475.

[10] G. Pieraccini, S. Furlanetto, S. Orlandini, G. Bartolucci, I. Giannini, S. Pinzauti, G. Moneti, Identification and determination of mainstream and

sidestream smoke components in different brands and types of cigarettes by means of solid-phase microextraction–gas chromatography–mass spectrometry, J. Chromatogr. A 1180 (2008) 138–150.

[11] A. R. Barnes, Determination of ceftazidime and pyridine by HPLC: application to a viscous eye drop formulation, J. Liq. Chromatogr. 18 (1995) 3117–3128.

[12] S. Saha, R. Mistri, B. C. Ray, Determination of pyridine, 2-picoline, 4-picoline and quinoline from mainstream cigarette smoke by solid-phase extraction liquid chromatography/electrospray ionization tandem mass spectrometry, J. Chromatogr. A 1217 (2010) 307–311.

[13] R. L. Chien, D. S. Burgi, Field amplified sample injection in capillary electrophoresis, J. Chromatogr. A 559 (1991) 141–152.

[14] C. X. Zhang, W. Thormann, Head-column field-amplified sample stacking in binary system capillary electrophoresis: a robust approach providing over 1000-fold sensitivity enhancement, Anal. Chem. 68 (1996) 2523–2532.

[15] N. Kaewchuay, K. Fukushi, A. Tsuboi, H. Okamura, K. Saito, T. Hirokawa, Simultaneous determination of pyridine-triphenylborane anti-fouling agent and its degradation products in paint-waste samples using capillary zone electrophoresis with field-amplified sample injection, Anal. Sci. 28 (2012) 1191–1196.

[16] T. Hattori, K. Fukushi, T. Hirokawa, Role of counter-ions in background electrolyte for the analysis of cationgenic weak electrolytes and amino acids in neutral aqueous solutions by capillary electrophoresis with electrokinetic injection, J. Chromatogr. A 1326 (2014) 130–133.

[17] T. Hattori, K. Fukushi, Highly sensitive tITP-CZE determination of L-histidine and creatinine in human blood plasma using field-amplified sample injection with mobility-boost effect, Electrophoresis 37 (2016) 267–273.

[18] R. L. Chien, D. S. Burgi, Sample stacking of an extremely large injection volume in high-performance capillary electrophoresis, Anal. Chem. 64 (1992) 1046-1050.

[19] F. Kitagawa, T. Kawai, K. Otsuka, On-line sample preconcentration by large-volume sample stacking with an electroosmotic flow pump (LVSEP) in microscale electrophoresis, Anal. Sci. 29 (2013) 1129–1139.

[20] P. Britz-McKibbin, D. D. Y. Chen, Selective focusing of catecholamines and weakly acidic compounds by capillary electrophoresis using a dynamic pH junction, Anal. Chem. 72 (2000) 1242–1252.

[21] J. B. Kim, Y. Okamoto, S. Terabe, On-line preconcentration of cationic analytes by dynamic pH junction in capillary electrophoresis, J. Chromatogr. A 1018 (2003) 251–256.

[22] K. Yasuno, K. Fukushi, CZE determination of sub-μM level of phenol in seawater using improved dynamic pH junction, Electrophoresis 37 (2016) 2496–2501.

[23] J. P. Quirino, S. Terabe, Exceeding 5000-fold concentration of dilute analytes in micellar electrokinetic chromatography, Science 282 (1998) 465–468.

[24] W. Grochocki, M. J. Markuszewski, J. P. Quirino, Three-step stacking by field-enhanced sample injection, sweeping, and micelle to solvent stacking

in capillary electrophoresis: Anionic analytes, J. Chromatogr. A 1442 (2016) 140–143.

[25] T. Hirokawa, H. Okamoto, B. Gaš, High-sensitive capillary zone electrophoresis analysis by electrokinetic injection with transient isotachophoretic preconcentration: electrokinetic supercharging, Electrophoresis 24 (2003) 498–504.

[26] Z. Xu, K. Kawahito, X. Ye, A. R. Timerbaev, T. Hirokawa, Electrokinetic supercharging with a system induced terminator and an optimized capillary versus electrode configuration for parts-per-trillion detection of rare-earth elements in CZE, Electrophoresis 32 (2011) 1195–1200.

[27] L. Y. Thanga, M. C. Breadmore, H. H. See, Electrokinetic supercharging in nonaqueous capillary electrophoresis for online preconcentration and determination of tamoxifen and its metabolites in human plasma, J. Chromatogr. A 1461 (2016) 185–191.

[28] L. Křivánková, P. Pantůčková, P. Boček, Isotachophoresis in zone electrophoresis, J. Chromatogr. A 835 (1999) 55–70.

[29] K. Fukushi, R. Yamazaki, T. Yamane, Determination of bromate in highly saline samples using CZE with on-line transient ITP, J. Sep. Sci. 32 (2009) 457–461.

[30] H. Okamoto, T. Hirokawa, N. Ikuta, Operational modes for transient isotachophoretic preconcentration-capillary zone electrophoresis and detectable concentration of rare earth ions, Electrophoresis 22 (2001) 3483–3489.

[31] K. Fukushi, Y. Nakayama, J. Tsujimoto, Highly sensitive capillary zone electrophoresis with artificial seawater as the background electrolyte and transient isotachophoresis as the on-line concentration procedure for simultaneous determination of nitrite and nitrate in seawater, J. Chromatogr. A 1005 (2003) 197–205.

[32] T. Okamoto, K. Fukushi, S. Takeda, S. Wakida, Determination of phosphate in seawater by CZE with on-line transient ITP, Electrophoresis 28 (2007) 3447–3452.

[33] P. Boček, P. Gebauer, M. Deml, Concept of the effective mobility of the hydrogen ion and its use in cationic isotachophoresis, J. Chromatogr. A 219 (1981) 21–28.

[34] C. Schwer, B. Gaš, F. Lottspeich, E. Kenndler, Computer simulation and experimental evaluation of on-column sample preconcentration in capillary zone electrophoresis by discontinuous buffer systems, Ana. Chem. 65 (1993) 2108–2115.

[35] V. Hruška, M. Jaroš, B. Gaš, Simul 5 – Free dynamic simulator of electrophoresis, Electrophoresis 27 (2006) 984–991.

[36] Ministry of the Environment (Government of Japan), [3] Aniline. https://www.env.go.jp/chemi/report/h14-05/chap01/03/03.pdf (accessed 17.05.02)

[37] Ministry of the Environment (Government of Japan), [16] Pyridine. https://www.env.go.jp/chemi/report/h16-01/pdf/chap01/02_2_16.pdf (accessed 17.05.02)

520 Fig. 1. Schematic diagram for tITP with an SIT: (A) initial state (a sample is
521 injected after the capillary is filled with BGE), (B) Migration of Na^+, An^+, and Py^+
522 to the cathode and that of AcO^- and Cl^- to the anode by electrophoresis, (C)
523 generation of SVZ and concentration of analytes by tITP, and (D) separation of
524 analytes. Other explanations are presented in the text.
525
526 Fig. 2. Electropherogram of a standard solution of An^+ and Py^+: (A) without tITP
527 and (B) tITP with an SIT. Analytical conditions: capillary, 62.4 cm total length
528 (50 cm effective length) and 50 μm I.D.; BGE, a mixture of 40 mM AcOH and 20
529 mM NaOH (pH 4.6); sample solution, a mixture of 5 mg/L An^+ and Py^+ (adjusted
530 to conductivity 100 mS/m by 10,000 mg/L NaCl); sample injection, vacuum (50
531 kPa for 1 s, 13 nL); SIT generation, 10 kV for 50 s; separation voltage, 25 kV;
532 wavelengths for detection, 200 and 254 nm. Analyte peak numbering: 1, Py^+; 2,
533 An^+; 3, SIT.
534
535 Fig. 3. Simulation results at 0 s (A, C) and 50 s (B, D) after voltage was applied:
536 (A) and (B) concentration profiles for AcO^-, Na^+, Cl^-, An^+, and Py^+ in the water,
537 the sample, and the BGE zones; (C) and (D) potential gradient and pH profiles in
538 the water, the sample, and the BGE zones. Other conditions are described in the
539 text.
540
541 Fig. 4. Electropherograms of sewage samples spiked with An^+ (0.050 mg/L) and
542 Py^+ (0.20 mg/L) (conductivity was adjusted to 100 mS/m by diluting with water).
543 (A) sewage sample S1; (B) sewage sample S2. Analytical conditions: BGE, a

mixture of 100 mM AcOH and 50 mM NaOH (pH 4.6); sample injection, vacuum (15 s, 190 nL); SIT generation, 10 kV for 80 s. Other electrophoretic conditions are identical to those used in Fig. 2.

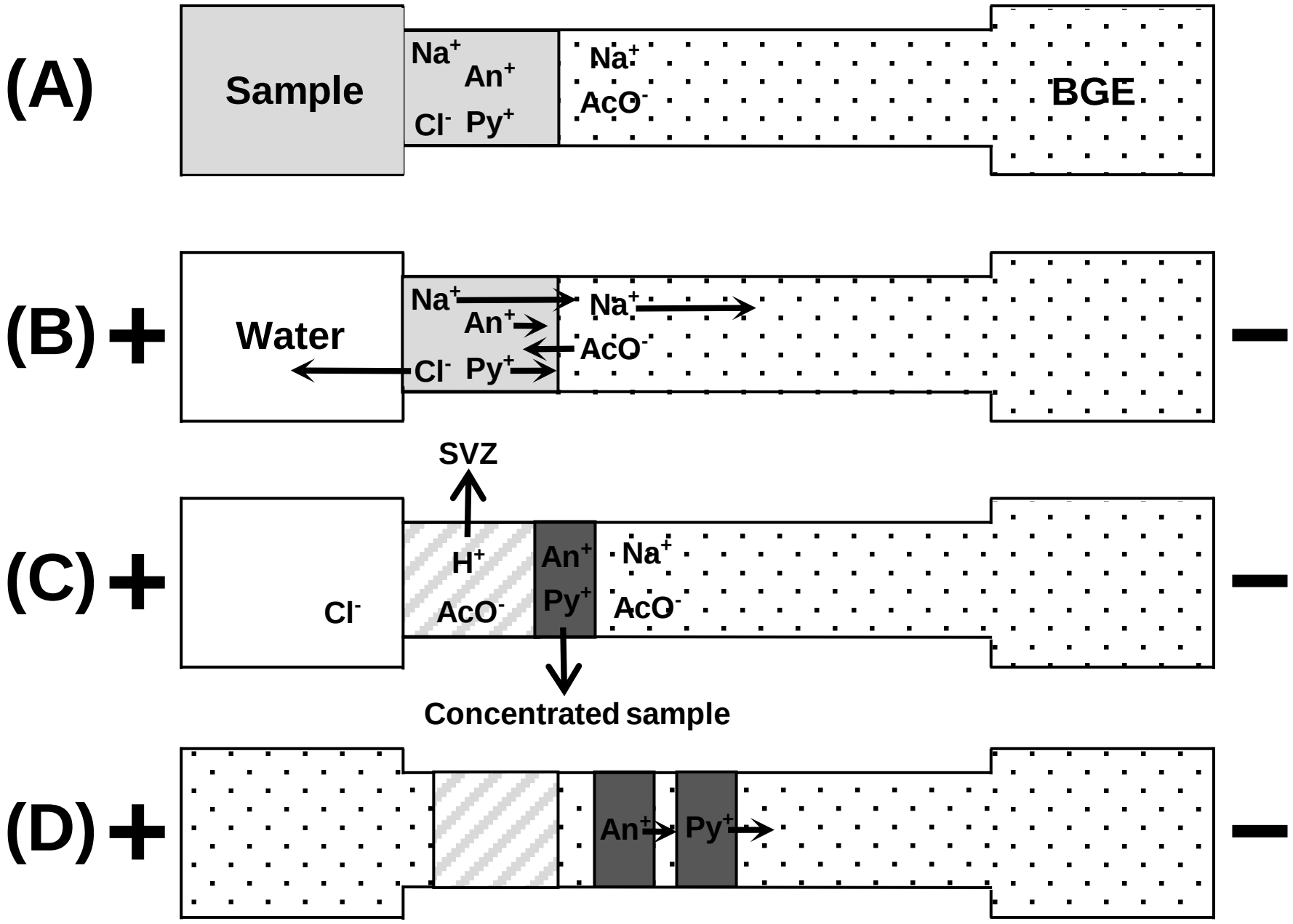
(A)
Sample
Na+
An+
Cl- Py+
Na+
AcO-
BGE
(B)
+
Water
Na+
An+
Cl- Py+
Na+
AcO-
−
(C)
+
SVZ
Cl-
H+
AcO-
An+
Py+
Na+
AcO-
−
Concentrated sample
(D)
+
An+
Py+
−

Fig. 1

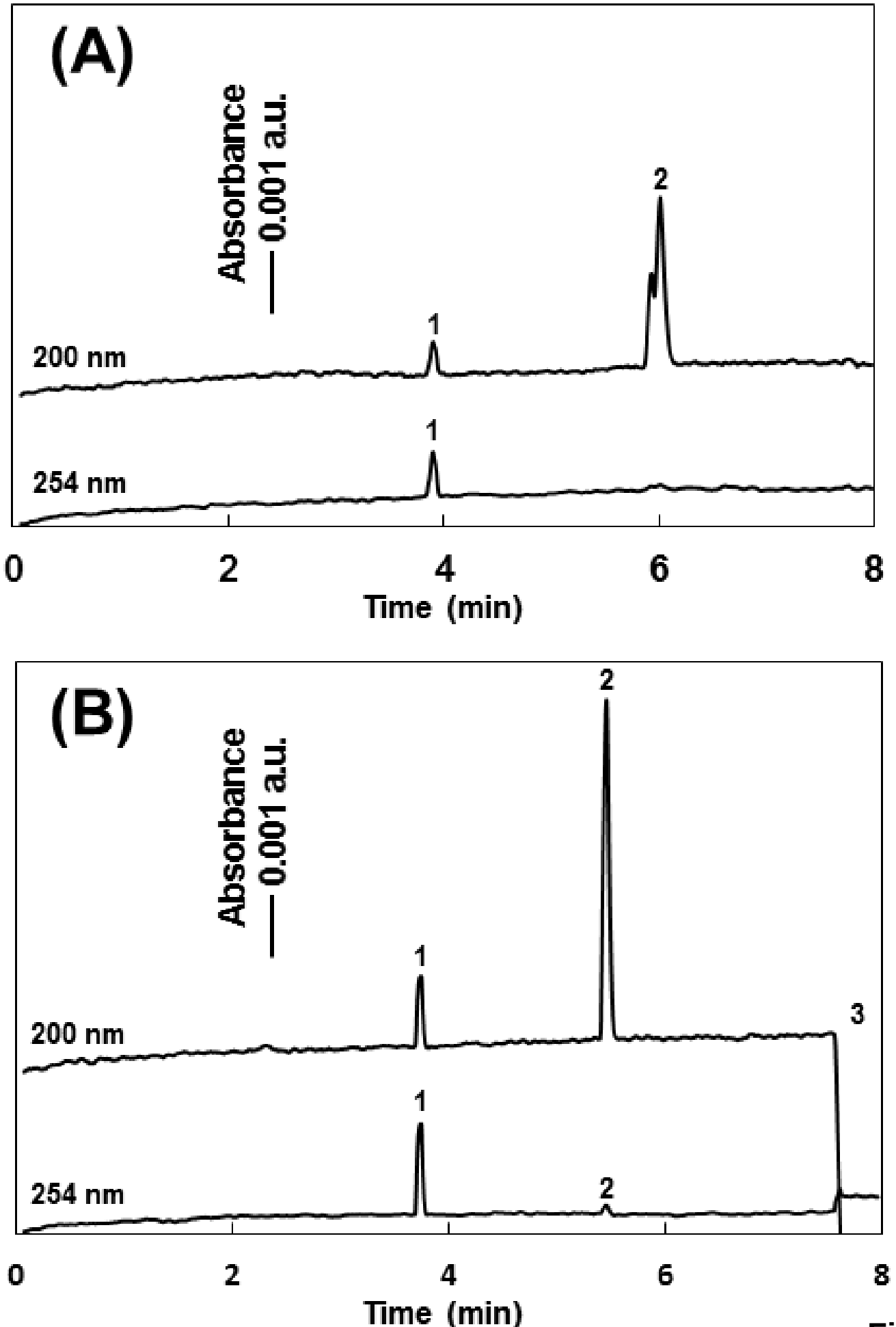
(A)
Absorbance
0.001 a.u.
200 nm
254 nm
1
2
0
2
4
6
8
Time (min)
(B)
Absorbance
0.001 a.u.
200 nm
254 nm
1
2
3
0
2
4
6
8
Time (min)

Fig. 2

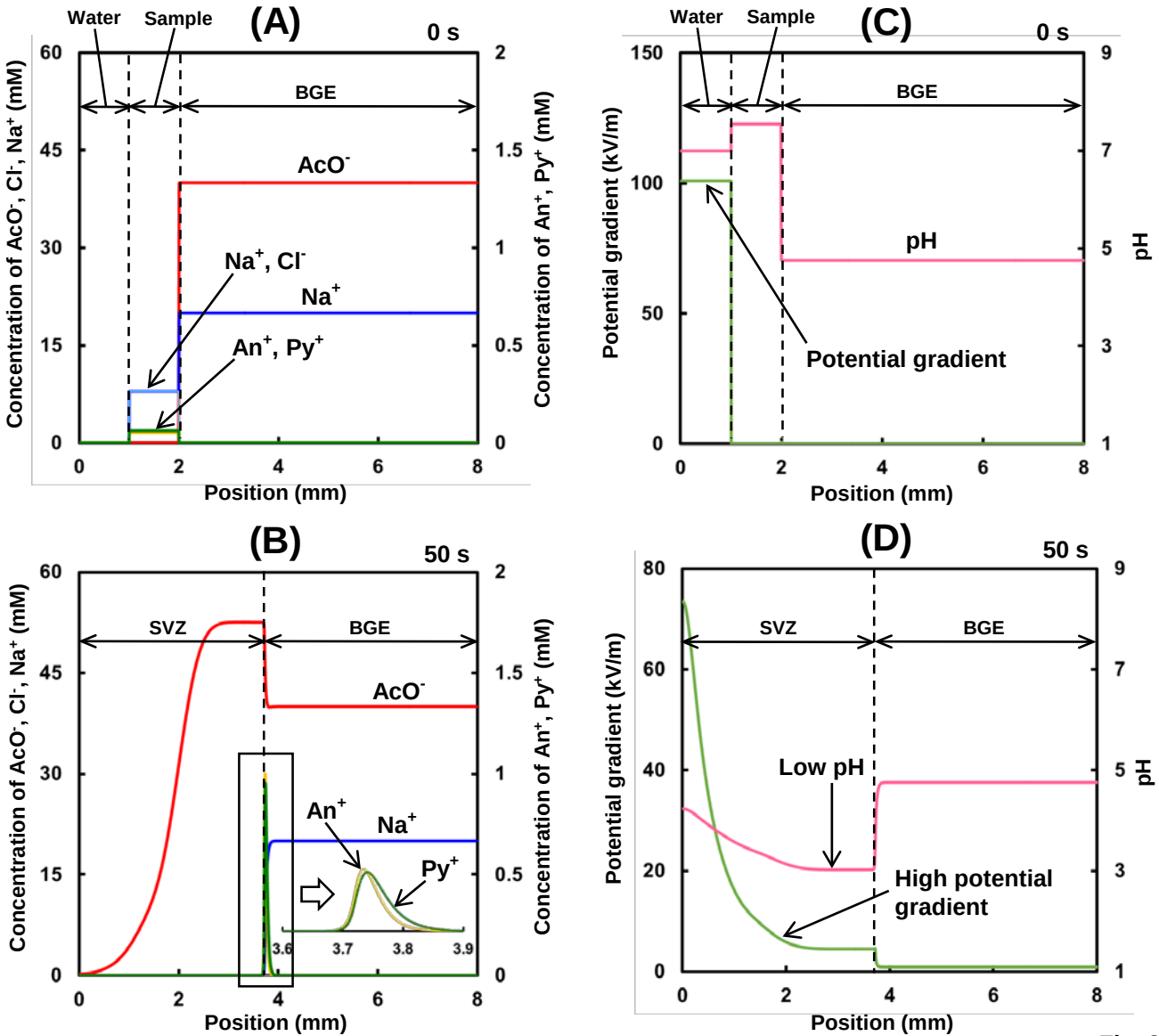
(A)
0 s
Water
Sample
BGE
AcO-
Na+, Cl-
Na+
An+, Py+
Concentration of AcO-, Cl-, Na+ (mM)
Concentration of An+, Py+ (mM)
Position (mm)
(C)
0 s
Water
Sample
BGE
pH
Potential gradient
Potential gradient (kV/m)
pH
Position (mm)
(B)
50 s
SVZ
BGE
AcO-
An+
Na+
Py+
Concentration of AcO-, Cl-, Na+ (mM)
Concentration of An+, Py+ (mM)
Position (mm)
(D)
50 s
SVZ
BGE
Low pH
High potential gradient
Potential gradient (kV/m)
pH
Position (mm)

Fig. 3

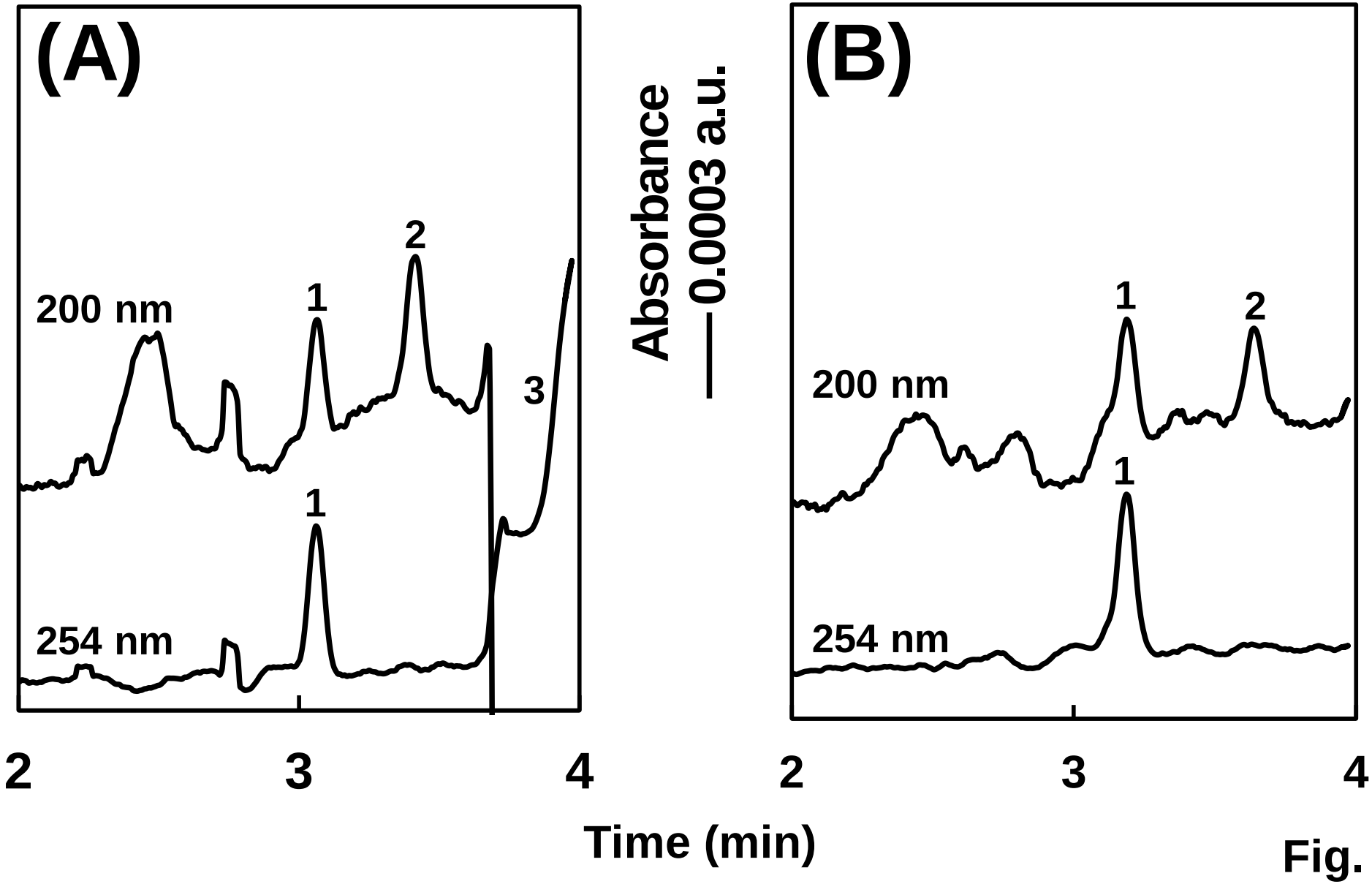
(A)
200 nm
1
2
3
254 nm
1
(B)
200 nm
1
2
254 nm
1
Absorbance
—0.0003 a.u.
2
3
4
2
3
4
Time (min)

Fig. 4

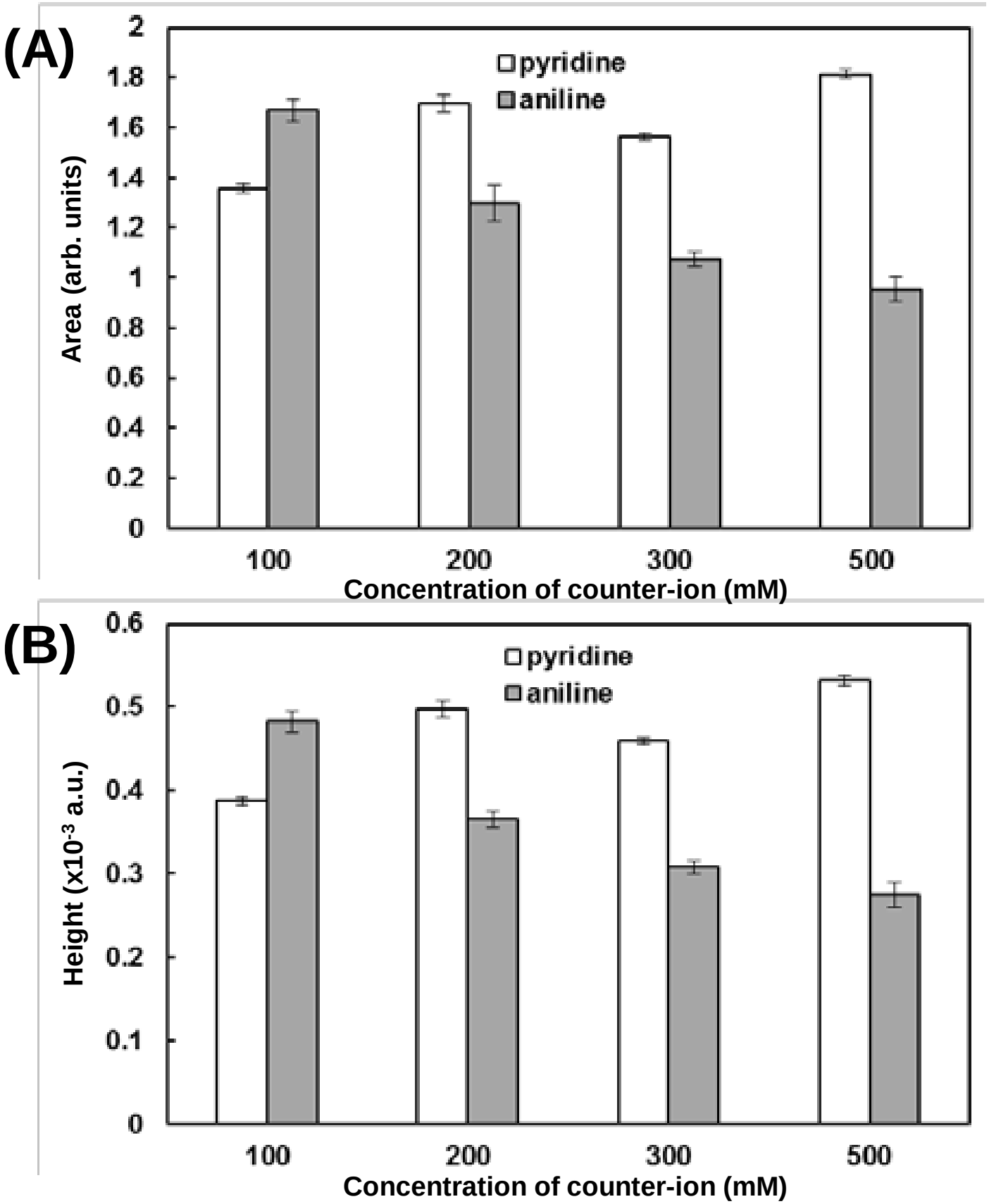

Fig. S1. Effect of counter-ion (AcO^-) concentration on the peak area (A) and the peak height (B) for An^+ and Py^+. Analytical conditions: BGE, a mixture of 100–500 mM AcOH and 50 mM NaOH; sample solution, a mixture of 0.5 mg/L An^+ and 2 mg/L Py^+ (adjusted to conductivity 100 mS/m by 10,000 mg/L NaCl). Other electrophoretic conditions are identical to those used in Fig. 2.

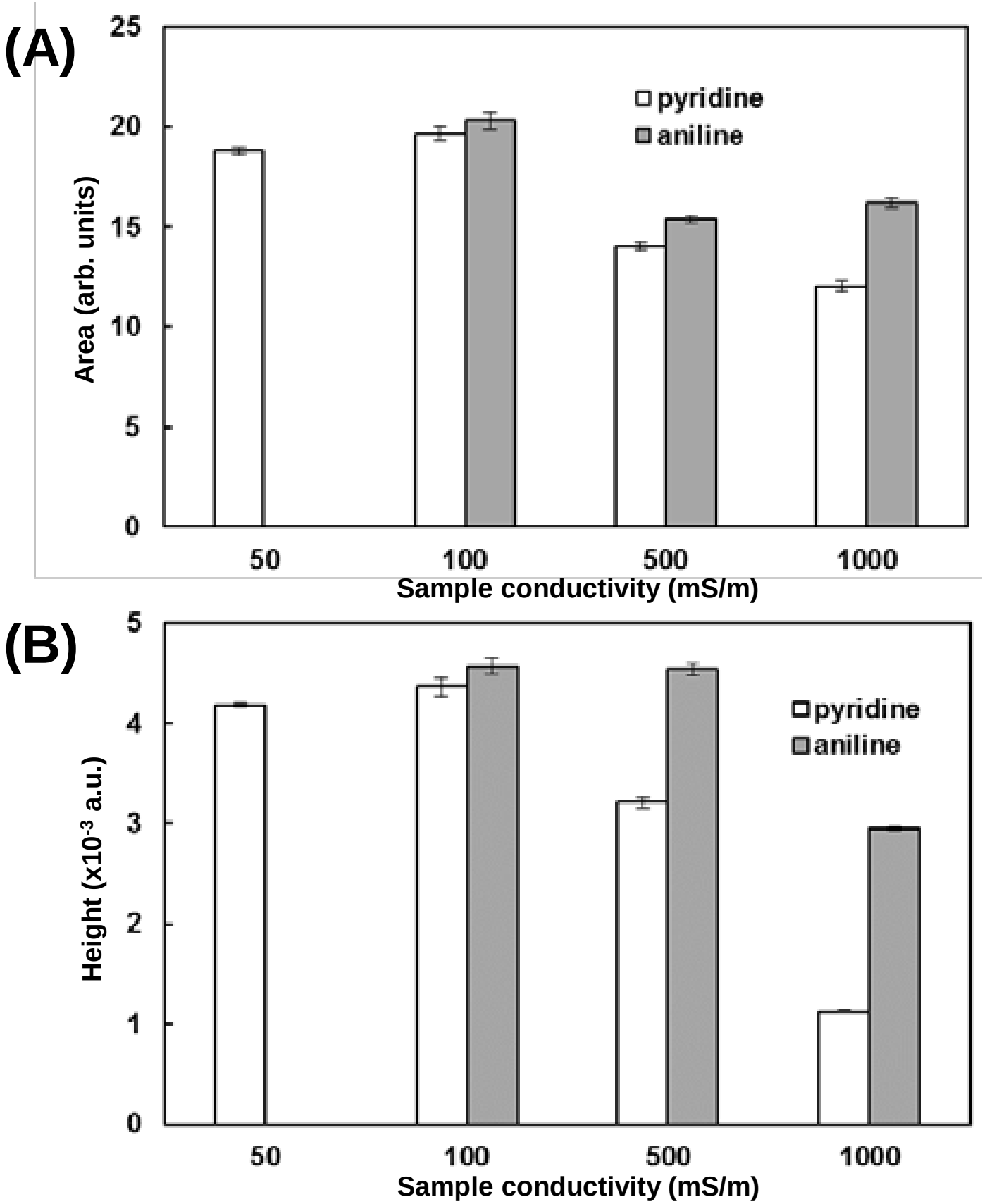

Fig. S2. Effect of sample conductivity on the peak area (A) and the peak height (B) for An^+ and Py^+. Analytical conditions: BGE, a mixture of 100 mM AcOH and 50 mM NaOH; sample solution, a mixture of 0.5 mg/L An^+ and 2 mg/L Py^+ (adjusted to conductivity 50–1000 mS/m by 10,000 mg/L NaCl). ; sample injection, vacuum (50 kPa for 15 s, 190 nL); SIT generation, 10 kV for 80 s. Other electrophoretic conditions are identical to those used in Fig. 2.

- Transient isotachophoresis with a system-induced terminator is proposed.
- No external terminating electrolyte is required.
- H^+ generated depending on the acid–base balance acts as the terminating ion.
- This on-line concentration method is applicable to high-conductivity samples.
- Limits of detection of aniline and pyridine are less than 50 micrograms per liter.